INSTITUTE OF PHYSICS PUBLISHING JOURNAL OF PHYSICS D: APPLIED PHYSICS

J. Phys. D: Appl. Phys. **40** (2007) 1138–1145 doi:10.1088/0022-3727/40/4/035

TSDC study of the glass transition: correlation with calorimetric data

J A Diego, J Sellarès , A Aragoneses, M Mudarra, J C Cañadas and J Belana

Departament de Física i Enginyeria Nuclear, Universitat Politècnica de Catalunya, Campus de Terrassa, c. Colom 11, E–08222 Terrassa, Spain

E-mail: jordi.sellares@upc.edu

Received 18 October 2006, in final form 14 December 2006
Published 2 February 2007
Online at stacks.iop.org/JPhysD/40/1138

Abstract

The glass transition in amorphous poly(ethylene terephthalate) is studied by thermally stimulated depolarization currents (TSDC) and differential scanning calorimetry (DSC). The ability of TSDC to decompose a distributed relaxation, as the glass transition, into its elementary components is demonstrated. Two fractional polarization techniques, windows polarization (WP) and non-isothermal windows polarization (NIW) are employed to assess the influence of thermal history in the results. The Tool–Narayanaswami–Moynihan model has been used to fit the TSDC spectra. The most important contributions to the relaxation comes from modes with a value of the non–linearity parameter (x) around 0.7. Activation energies yield by this model are located around 1 eV (96 kJ mol^{-1}) for polarization temperature (T_p) below 50 °C and they rise up to values higher than 8 eV (771 kJ mol^{-1}) as T_p increases (up to 80 °C). There are few differences between results obtained with WP and NIW but, nonetheless, these are discussed. The obtained kinetic parameters are tested against DSC results in several conditions. Calculated DSC curves at several cooling and heating rates can reproduce qualitatively experimental DSC results. These results also demonstrate that modelling of the non–equilibrium kinetics involved in TSDC spectroscopy is a useful experimental tool for glass transition studies in polar polymers.

1. Introduction

A glass is a material that behaves mechanically like a solid but has a disordered structure. In fact, glasses can be considered as super–cooled liquids that have acquired solid–like rigidity. The most common way of making a glass is by cooling the material from the melt fast enough to avoid crystallization. If a liquid is cooled in such a way, molecules will rearrange progressively more slowly as viscosity increases. Eventually the structure of the material will not be able to reach the equilibrium conformation fast enough to follow the cooling rate. This falling out of equilibrium is called the glass transition [1]. From this point of view, the glass transition would not be a true phase transition because all physical magnitudes would change in a continuous way. It has been suggested that there exists an underlying phase transition [1], but anyway the glass transition occurs across a narrow temperature range and therefore we can define a glass transition temperature (T_g). Below T_g only slow relaxation processes whereby the glass evolves spontaneously towards equilibrium can take place. This is known as structural relaxation or physical ageing. Due to the kinetic nature of the glass transition, T_g depends on the cooling rate, however this dependence turns out to be rather weak [2]. Anyway, to avoid confusion, we will denote the glass transition temperature at an almost null temperature change rate by T_g and we will use T_g^{dyn} to indicate the value at a given temperature change rate.

It is commonly accepted that the glass transition in polymers is a distributed process. We understand by distributed process a relaxation process that cannot be described in terms of a single relaxation time. In such processes, a distribution of relaxation times (DRT) is necessary to adequately describe its behaviour. A DRT is a set of elementary modes. On the one hand, each elementary mode of the DRT has a single

relaxation time. On the other hand, the superposition of all the elementary modes of the DRT gives the behaviour of the distributed process.

Calorimetric and dilatometric techniques have been widely employed to study the glass transition and several phenomenological models are used to model these results. In polar materials, dielectric spectroscopy techniques are also well suited to study the glass transition as the change in mobility of the main polymer chain, that occurs at T_g, will result in a change in the polarizability of the material. The relaxation response of a dielectric medium to an external electric field is known as dielectric relaxation. As a whole it is the result of the movement of dipoles (dipolar relaxation) and electric charges. Dynamic electrical analysis (DEA) is a well-known method that is based on the interaction of an external alternating field with the electric dipoles present in the sample. Although the aforementioned techniques are extensively employed in the study of the glass transition and related phenomena, some complexity arises in the interpretation of the results because of the distributed nature of the glass transition.

Although not as widely employed as DEA, thermally stimulated depolarization currents (TSDC) is another valuable technique to study dielectric relaxation. Its results are equivalent to those of DEA at very low frequencies (10^{-3}–10^{-4} Hz). TSDC has shown greater sensitivity in studying the glass transition of polymers. The most interesting feature of TSDC is its ability to study in its own each mode of a distributed process [3], as discussed below. Although TSDC is able to provide the relaxation time of each mode, it does not give information about the geometry of the reorientation processes, as, for example, multidimensional NMR [4], or the spatial heterogeneity of the relaxation, as, for example, non-resonant spectral hole burning [5].

A TSDC study can be described in the following way: the sample is taken from an initial temperature (T_i) to a polarization temperature (T_p) and is polarized for a polarization time (t_p) by a static polarizing field (E_p). Then it is cooled down to the storage temperature (T_s) and the field is switched off at a certain point during the cooling ramp. T_s is low enough so that depolarization of the sample takes place at a very low rate. By this way an electret is formed. The sample is then heated at a constant rate and the thermally activated depolarization current is recorded as a function of temperature to obtain a TSDC spectrum of the sample. Electret behaviour and TSDC have been widely described in the literature [6–8].

Let us consider the analysis of a distributed process by TSDC. If the polarizing field is on during a large portion of the cooling ramp (conventional polarization) many modes are recorded in the spectrum. In this case we have a distributed spectrum. A distributed spectrum can be resolved into elementary spectra if the electric field is switched off at a point of the cooling ramp near T_p or even at the beginning of the cooling ramp (windowing polarization (WP) [9–11]. An elementary spectrum can be described in terms of a single relation time and corresponds to an elementary mode of the distribution process. It can be obtained if the thermal window is narrow enough.

One of the relaxations that can be detected by TSDC is the α relaxation, which is the dielectric manifestation of the glass transition. In TSDC data, the α peak has its maximum at T_g^{dyn} [12]. Unlike in other relaxations [13–15], the Arrhenius law

$$\tau(T) = \tau_0 \exp\left(\frac{E_a}{RT}\right) \tag{1}$$

does not work properly when the system is close to the glass transition because cooperative phenomena are involved [16]. The temperature dependence is better described by a Vogel–Tammann–Fulcher (VTF) type expression,

$$\tau(T) = \tau_0 \exp\left[\frac{E_w}{R(T - T_\infty)}\right], \tag{2}$$

where T_∞ is the temperature at which molecules would 'freeze' and the relaxation time of the system would become infinite. It can be shown that this model is equivalent to the Williams–Landel–Ferry equation.

In spite of the fact that the VTF model describes the α relaxation better than the Arrhenius model, well-known non–linear phenomena like thermal history effects and physical ageing cannot be explained by this model. As a consequence, the parameters obtained through the VTF model will depend to some extent on the thermal history of the sample.

In order to model such memory effects, at least an additional parameter that takes into account the structural conformation of the system must be introduced. An appropriate parameter is the fictive temperature T_f. The fictive temperature of a non-equilibrium system is the temperature of an equilibrium system with the same structural conformation. The simplest extension to the Arrhenius model that incorporates this parameter is the Tool–Narayanaswamy–Moynihan (TNM) model [17]

$$\tau(T, T_f) = \tau_0 \exp\left(\frac{xE_a}{RT}\right) \exp\left[\frac{(1-x)E_a}{RT_f}\right]. \tag{3}$$

In this model the separation between T and T_f is introduced through a non–linearity parameter x ($0 \leqslant x \leqslant 1$). The other two parameters are the pre–exponential factor τ_0 and the activation energy E_a. The evolution of T_f with time and temperature is introduced assuming an ideal-viscous return to equilibrium that depends on the relaxation time $\tau(t)$ by the equation

$$\frac{dT_f}{dt} = \frac{1}{\tau(t)}(T - T_f). \tag{4}$$

Equations (3) and (4) are coupled. Their exact solution can be expressed as

$$T_f(t) = T(t) - \phi[z(t)][T_f(0) - T(0)] - \int_0^t \frac{dT(t')}{dt'}\phi[z(t) - z(t')]\,dt', \tag{5}$$

where the reduced time (z) is

$$z(t) \equiv \tau_0 \int_0^t \frac{dt'}{\tau(t')}dt' \tag{6}$$

and the response function ϕ is, in the case of elementary relaxations,

$$\phi(t) \equiv \exp\left(-\frac{t}{\tau_0}\right). \tag{7}$$

Numerical methods are required to integrate equations (5) and (6). Nevertheless, they are often found in the literature since they can be used in some DRT implementations, such as the Kohlrausch–Williams–Watts (KWW) distribution, just changing equation (7) for a modified response function [18].

In this work we present a TSDC based analysis that is able to characterize structural relaxation near the glass transition. We will take advantage of possibilities of TSDC to determine the DRT more clearly than with the calorimetric methods. Using this analysis we will obtain an acceptable correlation with DSC data. Throughout, the similarities and differences with current approaches will be stressed.

2. Experimental

Experiments were carried out on commercial poly(ethylene terephthalate) (PET), Hosta-PET®, 100 μm thick sheets. Samples were almost amorphous with less than 3% crystallinity degree. From previous works [19] it was known that for this material T_g^{dyn} is approximately 80 °C at 2.5 °C min^{-1} and that crystallization does not take place under 100 °C.

Circular samples were prepared for current measurements coating 1 cm diameter Al electrodes on both sides of the sheet by vacuum deposition. Thermally stimulated currents have been carried out in a non-commercial experimental setup, controlled by an Eurotherm–2416 temperature programmer. Temperature, during measurements, was measured to an accuracy of 0.1 °C by a J–thermocouple located inside the electrodes (in direct contact with the sample). A Keithley–6512 electrometer has been employed for the current intensity measurements.

The TSDC experiments were performed using the null width polarization windowing method, a particular case of the windowing polarization (WP) technique (see section 1) and the non-isothermal windowing polarization (NIW) technique. All the TSDC experiments begin at T_i above T_g to ensure that there is no influence from previous thermal history.

In WP the sample is then cooled to the polarization temperature (T_p). Once the sample is at T_p, a polarizing potential (V_p) is applied after a time t_d. V_p is applied for a polarizing time (t_p). Once t_p is over, the polarizing potential is switched off and the sample is cooled until the storage temperature (T_s) is attained. The sample remains at T_s for a short storage time (t_s) and then it is heated at a constant rate while the TSDC discharge is recorded. In all WP experiments, $T_i = 95$ °C, $V_p = 800$ V, $t_d = 2$ min, $t_p = 5$ min, $T_s = 30$ °C, $t_s = 5$ min and the cooling and heating rate is 2.5 °C min^{-1}.

To avoid the different thermal history in each measurement, inherent to the WP method, the NIW method was also used. In this method the sample was continuously cooled from T_i to T_s and the polarizing field was applied during the cooling ramp when the temperature of the sample reaches T_p and switched off $\Delta T = 2$ °C below T_p. As in WP experiments, in NIW experiments $T_i = 95$ °C, $V_p = 800$ V, $T_s = 30$ °C, $t_s = 5$ min and the cooling and heating rate is 2.5 °C min^{-1}.

A spectrum using conventional polarization was obtained using a polarizing potential $V = 800$ V. The sample was cooled from a temperature above $T_p = 95$ °C to $T_s = 30$ °C. The electric field was on between 95 and 40 °C, without isothermal polarization. This broad temperature range allows us to polarize most modes of the mechanism. The sample was at T_s for 5 min and then it was heated while the TSDC was recorded. The cooling and heating rates were the same as in the other experiments (2.5 °C min^{-1}).

The calorimetric measurements were made with a Mettler TC11 thermoanalyser equipped with a Mettler–20 differential scanning calorimeter module. The calorimeter has been previously calibrated with metallic standards (indium, lead, zinc). DSC curves were obtained from 8 to 20 mg samples, sealed in aluminium pans. All DSC experiments begin at 90 °C, clearly above T_g but low enough so crystallization does not take place. Samples are cooled to 40 °C and heated again to 90 °C. The values 1.25, 2.5 and 5 °C min^{-1} have been employed for the cooling and heating rates.

3. Results and discussion

3.1. Modelling procedure

If we assume that structural relaxation at the glass transition and dielectric α relaxation are two manifestations of the same physical phenomenon, we can use TSDC together with WP to track each mode of the distributed relaxation independently of the other ones. This is a huge difference with other techniques such as DSC that do not have this ability. It also suggests a possible way to model the distribution of relaxation times that can take advantage of this feature of TSDC, although its validation should come from comparison with experimental data.

According to this approach, each mode of the structural relaxation evolves independently from the other ones. This results in as many equations (3) and (4) as modes of the process, each one with its own fictive temperature

$$\tau_i(t) = \tau_{0i} \exp\left[\frac{x_i E_{ai}}{RT(t)}\right] \exp\left[\frac{(1-x_i)E_{ai}}{RT_{fi}(t)}\right], \tag{8}$$

$$\frac{dT_{fi}(t)}{dt} = \frac{1}{\tau_i(t)}[T(t) - T_{fi}(t)]. \tag{9}$$

The relaxation time distribution is characterized by the sets $\{g_i]\}$, $\{\tau_{0i}\}$, $\{E_{ai}\}$ and $\{x_i\}$. $\{g_i\}$ is a set of normalized weights that stand for the relative contribution of each mode of the relaxation. $\{\tau_{0i}\}$ and $\{E_{ai}\}$ are the pre–exponential factors and the activation energies of the different modes of the relaxation.

There are several differences between this approach and the usually employed method that consists of a combination of the TNM model and the KWW distribution [18]. When the KWW distribution is used, the relaxation is characterized only by three parameters (an activation energy E_a, a pre-exponential factor τ_0 and a non–exponential relaxation parameter β). This distribution may be appropriate to model data obtained by techniques that cannot resolve individual modes of the relaxation but more flexibility is desired to take the maximum advantage of TSDC. Another difference is that there is a single T_f when the TNM model is combined with the KWW distribution, while in the presented approach all the modes have their own T_{fi}.

The intensity current that corresponds to an elementary mode of the α relaxation during the heating ramp is given by [20]

$$I_i(t) \propto \exp\left[-\int_{t0}^{t} \frac{dt'}{\tau_i(t')} - \ln[\tau_i(t)]\right], \qquad (10)$$

where t_0 is the initial time of the heating ramp. It is obtained by assuming that the polarization of mode i follows a first–order relaxation process determined by the relaxation time τ_i. This dielectric relaxation time is considered to be the same as the structural relaxation one.

The intensity of a thermally stimulated discharge current is usually acquired as a function of T. For this reason, sometimes a variable change between t and T has to be performed. This presents no problem since the thermal history of the experiment $T(t)$ is known.

The key of the calculation is obtaining $\tau_i(t)$. In fact, it would be more accurate to express it as $\tau_i[T(t), T_{fi}(t)]$, since the time dependence comes through $T(t)$ and $T_{fi}(t)$. The main difficulty to calculate $\tau_i(t)$ is that it depends on $T_{fi}(t)$ which in its turn depends on $\tau_i(t)$, as it can be seen in equation (9). A possible approximation would be to consider that T_{fi} is constant in the glassy state [21]. Although it may be enough to discuss some features of the experimental plots, this approximation is too crude to calculate realistic TSDC or DSC plots.

Two different numerical approaches have been tested to obtain $\tau_i(t)$: (a) numerical resolution of equations (8) and (9) (b) numerical integration of equation (5), particularized for each mode. The coincidence in the results of both the methods demonstrates the validity of the numerical algorithms.

In this work, the parameters that correspond to each mode are obtained fitting a calculated depolarization current $I_i(T)$ to experimental TSDC/WP and TSDC/NIW data by means of χ^2 minimization. The routines used are described by other authors [22].

As mentioned above, validation of the assumptions that have been employed should come from comparison with experimental data. The calorimetric DSC curves can be calculated from the fictive temperature $T_{fi}(t)$ obtained for each mode during the calculation process. A general fictive temperature is defined by

$$T_f(t) = \sum_{i=1}^{n} g_i T_{fi}(t), \qquad (11)$$

and from this quantity the normalized calorific capacity is obtained by [23]

$$C_p^n = \frac{dT_f}{dT}. \qquad (12)$$

This result can be compared with experimental DSC scans after they are normalized.

3.2. Analysis of TSDC data

A spectrum obtained by conventional polarization, as specified in section 2, is presented in figure 1. The broad and asymmetric peak corresponds to the α relaxation, that is a distributed process. It has a maximum at 79 °C. The peak contains the contribution of most modes of the α relaxation as the polarizing field has been applied in a broad temperature range. It can be resolved in its elementary components using fractional polarization techniques, such as WP or NIW, as explained previously.

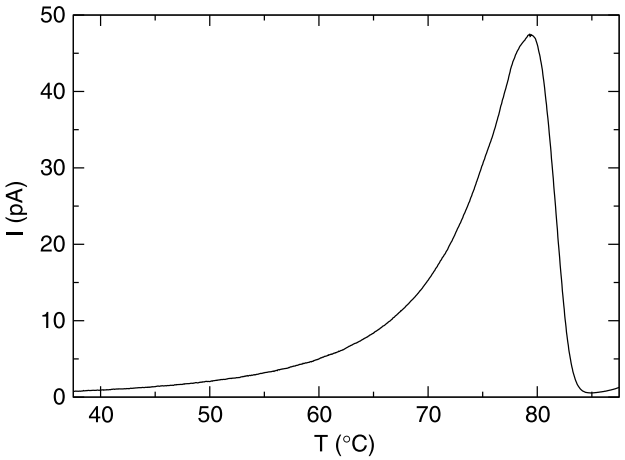

Figure 1. Experimental TSDC spectra of the α relaxation of PET obtained by conventional polarization.

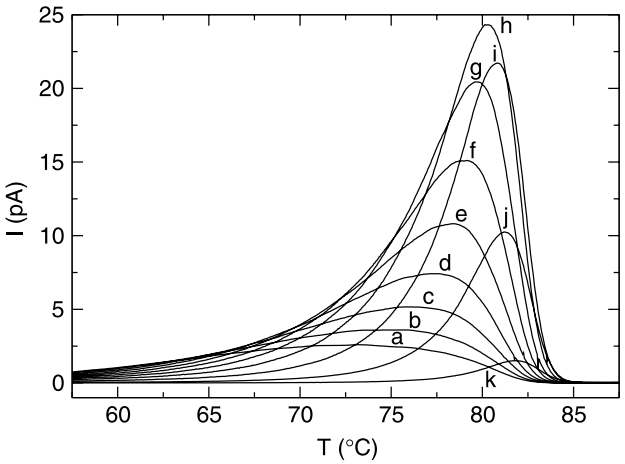

Figure 2. Experimental TSDC spectra of the α relaxation of PET obtained by WP at different T_p: from 60 °C (curve a) to 80 °C (curve k) in 2 °C increment steps.

The sets $\{g_i\}$, $\{\tau_{0i}\}$, $\{E_{ai}\}$ and $\{x_i\}$ are obtained analysing a set of TSDC/WP or TSDC/NIW spectra that correspond to several polarization temperatures. We have employed an equispaced set of polarization temperatures from $T_p = 40$ °C up to $T_p = 86$ °C in 2 °C steps to obtain a representative set of parameters. The same set of polarization temperatures has been used for WP and NIW experiments.

Figure 2 shows a subset of these spectra, obtained by WP, corresponding to the main modes that reproduce the relaxation. The α dipolar peak presents its maximum value of intensity for $T_p = 74$ °C, at a temperature $T_m = 80$ °C. We will refer to this polarization temperature as the optimal polarization temperature (T_{po}). As T_p is increased or decreased from this value, the peak maximum shifts in temperature. This clearly indicates the distributed nature of the process. Each spectra records a mode of the relaxation and the analysis of all of them allows us to study the distribution.

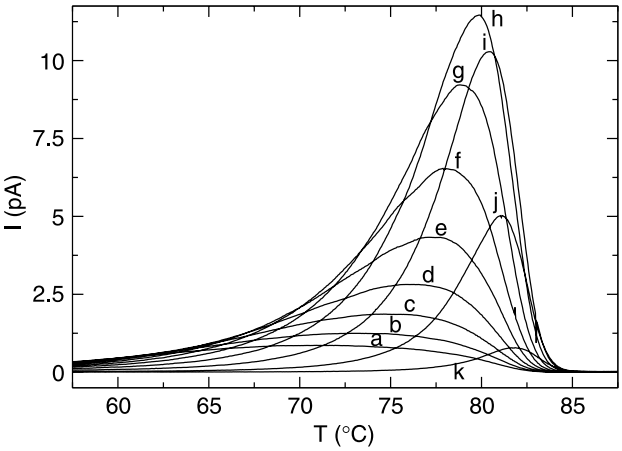

Figure 3. Experimental TSDC spectra of the α relaxation of PET obtained by NIW at different T_p: from 60 °C (curve a) to 80 °C (curve k) in 2 °C increment steps.

To obtain spectra that correspond as much as possible to a single elementary mode, a small polarization time has been used ($t_p = 5$ min) and the electric field has been switched off just before the start of the cooling ramp. In this way we limit the contribution from modes with a relaxation time different from the one that corresponds to the main mode that is being polarized. Moreover, physical ageing during the isothermal polarizing stage is minimized and as a consequence polarization is more sharply focused on a single mode. Anyway, there is the possibility that more than one mode of the relaxation process can be recorded in each measurement. To analyse if this effect appreciably affects the results, a set of TSDC spectra was obtained by polarizing the NIW method with $\Delta T = 2$ °C (see section 2), using the same polarization temperatures. The thermal history of a NIW experiment is simpler, at the expense of a lower intensity signal.

The NIW spectra are presented in figure 3. There are no appreciable differences from the spectra obtained by WP, as it would be expected if both the methods are activating the same elementary mode of the relaxation. The overall intensity of the peaks is lower since in NIW experiments the polarizing field is on for a shorter amount of time. The T_{po} is the same as in WP experiments ($T_{po} = 74$ °C) and its maximum is placed at the same temperature ($T_m = 80$ °C).

τ_{0i}, E_{ai} and x_i for each mode can be obtained fitting numerical calculations of $I_i(t)$ (Equation (10)) to experimental data. First, fits have been performed setting these three parameters free. Unlike τ_{0i} and E_{ai}, x_i values did not show a broad distribution. For this reason, the mean values were calculated ($x = 0.683$ for WP and $x = 0.713$ for NIW) and the fittings were performed again fixing the x parameter to these values and setting free only τ_{0i} and E_{ai}. In the following, we will omit the subindex i to lighten the notation. Tables 1 and 2 reproduce the parameters obtained in this way for each curve. The curves corresponding to lower polarization temperatures have been neglected as their intensity is very low and, as a consequence, the evaluation of their parameters becomes uncertain.

As a general trend, in the case of WP, we can see that $\log_{10}(\tau_0/1\text{s})$ decreases as T_p increases, with values ranging from -22.8 to -108. The activation energy increases as T_p does so, with values from 1.70 eV to 7.67 eV. The values obtained from the NIW spectra are comparable and show a similar behaviour.

Table 1. Kinetic parameters obtained in the fitting process of TSDC/WP spectra to the TNM model. $x = 0.683$ for every mode.

	T_p (°C)	$\log_{10}(\tau_0/1\text{s})$	E_a (eV)	g/g_{max}
a	60	−22.8	1.70	0.298
b	62	−25.5	1.89	0.379
c	64	−30.1	2.21	0.470
d	66	−35.8	2.61	0.579
e	68	−43.0	3.12	0.713
f	70	−50.6	3.65	0.856
g	72	−60.5	4.34	0.977
h	74	−70.8	5.07	1.00
i	76	−80.8	5.77	0.794
j	78	−93.8	6.70	0.330
k	80	−108	7.67	0.0442

Table 2. Kinetic parameters obtained in the fitting process of TSDC/NIW spectra to the TNM model. $x = 0.713$ for every mode.

	T_p (°C)	$\log_{10}(\tau_0/1\text{s})$	E_a (eV)	g/g_{max}
a	60	−20.2	1.53	0.235
b	62	−23.5	1.76	0.301
c	64	−27.8	2.06	0.390
d	66	−33.2	2.43	0.504
e	68	−40.1	2.92	0.652
f	70	−48.8	3.52	0.820
g	72	−58.7	4.22	0.973
h	74	−71.6	5.12	1.00
i	76	−85.1	6.08	0.762
j	78	−98.1	7.00	0.330
k	80	−111	7.93	0.0472

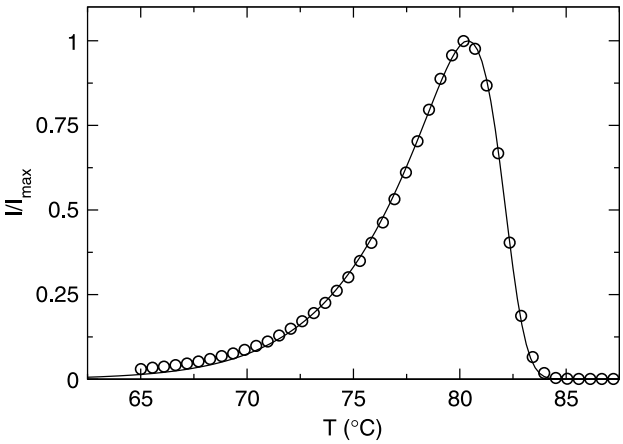

Figure 4. Calculated (continuous) and experimental (circles) TSDC spectrum of PET for $T_p = 74$ °C (fitted values: $\tau_0 = 1.46 \times 10^{-71}$ s, $E_a = 5.07$ eV, $x = 0.683$).

Figure 4 shows a comparison between the experimental curve polarized by WP at $T_p = 74$ °C and the curve calculated from the fit results. An overall good agreement can be observed. Similar plots can be obtained for the other modes, either from WP or NIW experiments. In all the cases, fitting to the TNM model, we are able to reproduce closely the experimental results.

The relative weight of each contribution, g, is roughly proportional to the polarization of the peak which, at its turn, is

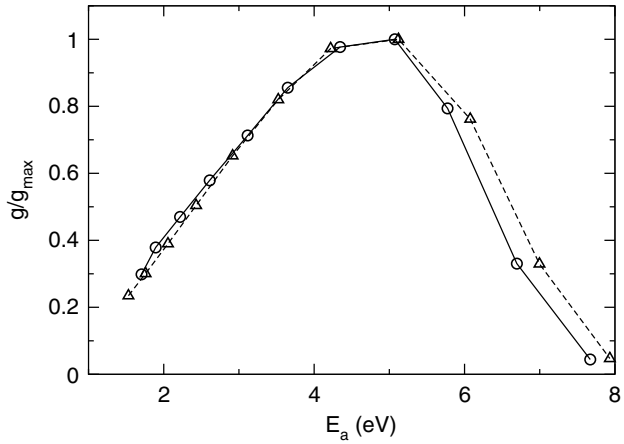

Figure 5. Obtained distribution of weights g_i for each analysed mode of the α relaxation. Polarization technique: WP (circle, continuous line), NIW (triangle, dashed line).

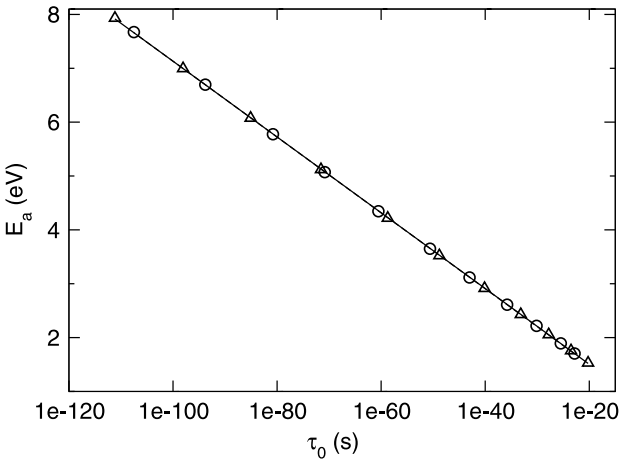

Figure 6. Compensation plot: WP (circle, dashed line), NIW (triangle, dashed line).

proportional to its area. To take into account the dependence of polarizability with temperature, the area is multiplied by T_p to obtain g [3]. Figure 5 shows the relative distribution of weights for the α relaxation, calculated in this way. The distributions obtained by WP and by NIW are very similar, especially when $T_p < T_{po}$.

There is a linear relationship between $\log_{10}(\tau_0)$ and E_a that can be appreciated in figure 6. This relationship is known as compensation law [3]. The concordance between the WP and NIW linear regression parameters is very accurate. For WP the intersect is $A = 0.0930$ eV and the slope is $B = -0.0702$ eV while for NIW the intersect is $A = 0.0979$ eV and the slope is $B = -0.0705$ eV. For both regression coefficients, the first five significant figures are nine. Due to this relationship, the distribution of g in terms of $\log_{10}(\tau_0)$ has the same shape as in terms of E_a if the x axis is inverted.

The slight differences between the WP and NIW results in figure 5 give us some clues about the merits of both the polarization techniques. Although the compensation plots shown in figure 6 are almost identical, the WP and NIW modes are on different points on the compensation line. It can be interpreted that in spite of giving almost elementary spectra, both the methods do not focus on exactly the same mode for a given T_p. In figure 5 it can be seen that the reason for this discrepancy is different whether T_p lies above or below T_{po}.

For polarization temperatures above T_{po}, WP weights (figure 5) lie below the corresponding values obtained by the NIW method. This behaviour can be explained if we assume that significant depolarization occurs in the WP method in the meantime while the polarizing field is switched off and the cooling ramp effectively starts. Due to the characteristic thermal inertia of the used experimental setup, roughly 30 s pass before the cooling rate reaches 2.5 °C min^{-1}. This implies a considerable depolarization taking into account that the temperature of the sample is above the static T_g.

Therefore, weights obtained by means of WP experiments can be undervalued for these modes. The NIW experiments do not present this effect because the field is applied during the cooling ramp.

Below T_{po}, the weights provided by both the methods agree better. They tend to lie in the same curve but at different points. Physical ageing during polarization in the WP curves is the most probable cause of this trend. The reduction of free volume helps to maintain the polarization of the activated modes once the polarizing stage is over. For this reason, there is a better agreement between the weight curves obtained by means of both the methods.

It can be observed that, for these polarization temperatures, a mode with a higher E_a is activated by WP, when the same T_p as with NIW is employed. Again, physical ageing of the sample during polarization can explain this behaviour. Restriction of chain mobility during ageing shifts the depolarization peak to higher temperatures [24], delivering higher activation energies. We can see as well that this shift in E_a is more pronounced for T_p around 10 °C below T_{po} and decreases as T_p approaches T_{po} as expected.

All in all, both the polarization methods give comparable results when they are applied to the entire relaxation but the lack of physical ageing or isothermal depolarization makes the NIW results easier to understand and a little bit more reliable. For this reason, in the following lines we will centre our discussion on the NIW results, although the WP results are similar and lead to the same conclusions in all cases.

In figure 7, T_p is plotted versus E_a for the NIW curves. It can be seen that the increase of E_a is small for low T_p and speeds up as T_p reaches higher values. This trend is confirmed by more qualitative results obtained fitting the curves polarized at lower T_p (presented as error bars due to uncertainty in the fittings). We can infer, then, that the activation energies of the low E_a modes of the relaxation should not be less than 1 eV.

3.3. Comparison with DSC results

Justification of the employed method should come from the comparison of its results with experimental data. For this purpose, the calorimetric DSC curves of the glass transition were calculated from equations (11) and (12). The relaxation has been modelled using the parameter values presented in Table 2, that correspond to 11 modes.

Experimental plots have been normalized as follows. The low–temperature part of the experimental plot has been fitted by linear regression to a line and this line has been

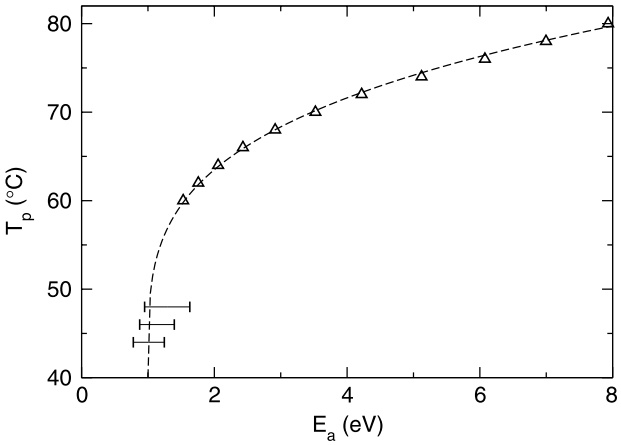

Figure 7. Relation between E_a and T_p for NIW curves. The dashed line is a guide for the eye.

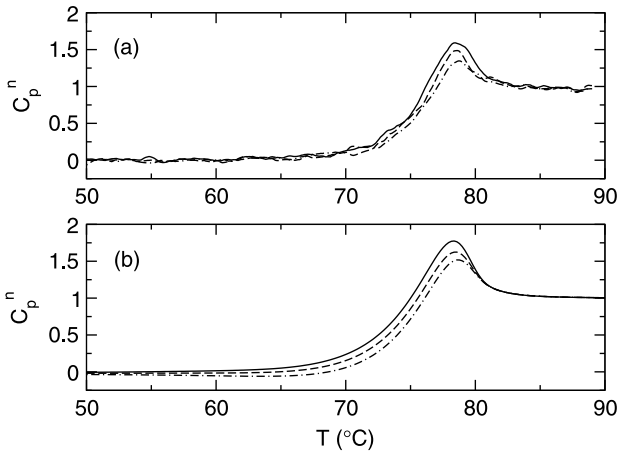

Figure 8. C_p^n for 2.5 °C min^{-1} heating rate. Cooling rate is 1.25 °C min^{-1} (continuous), 2.5 °C min^{-1} (dashed) and 5 °C min^{-1} (point–dashed). (*a*) Experimental DSC curves. (*b*) Calculated curves.

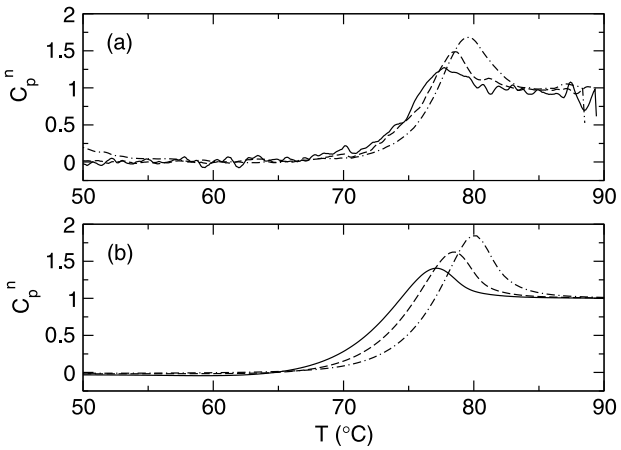

Figure 9. C_p^n for 2.5 °C min^{-1} cooling rate. Heating rate is 1.25 °C min^{-1} (continuous), 2.5 °C min^{-1} (dashed) and 5 °C min^{-1} (point–dashed). (*a*) Experimental DSC curves. (*b*) Calculated curves.

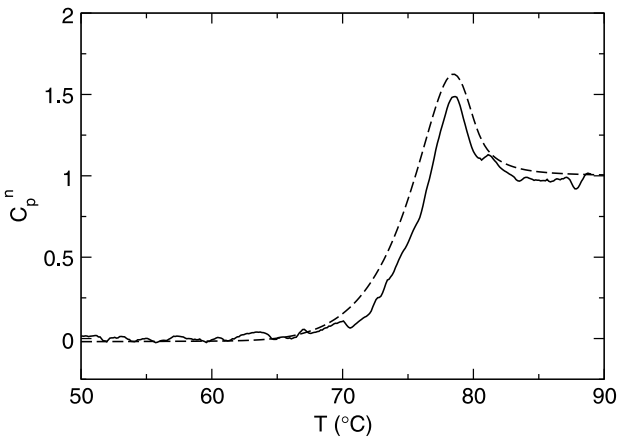

Figure 10. Comparison of C_p^n obtained by DSC (continuous) and by calculation (dashed). Cooling and heating rate 2.5 °C min^{-1}.

subtracted from the entire plot. Then, the experimental data has been multiplied by a constant factor in order to make the high-temperature end of the plot equal to one. The same normalization parameters have been employed for curves with the same heating rate.

Calculated DSC curves are plotted in figures 8 and 9, together with the corresponding experimental results. An offset of 3.1 °C has been subtracted from all the temperatures of the calculated curves to fit their maxima to the experimental ones. The more probable cause of this temperature offset may be associated with some thermal gradient in the TSDC setup, although it could also be due to limitations of the employed approach. Once the temperature offset has been corrected, we can appreciate qualitatively good agreement in both the cases. In figure 8 we can see the effect of changing the cooling rate. There is a higher enthalpy recovery for lower cooling rates, that is reproduced by the model. In Figure 9 the effect of changing the heating rate is shown. In this case the enthalpy recovery is more pronounced for higher heating rates. This behaviour is also reproduced by the model. Dependence of the temperature where the transition occurs with the change in the heating or cooling rate is reproduced by the model in both the cases. It should be noted that in the limit $x = 1$ (which is equivalent to the Arrhenius model) there would be no endothermic peak in the calculated DSC curves. This is a qualitative feature given by the TNM model.

In figure 10 the experimental and the calculated DSC curves are compared side by side. Some differences between them can be observed. The experimental endothermic peak, once normalized, is less pronounced than the predicted one. This effect could be related to thermal inertia in the DSC sample. Also, the inclusion of low-E_a-modes in the calculation would lead to a better concordance in the part of the curve that corresponds to the glassy state.

4. Conclusions

It has been known for a long time that the α relaxation is the dielectric manifestation of the glass transition [12]. Following this idea, in this work we suggest a method to study the glass transition using TSDC and we show how to correlate these results with DSC data by means of the TNM model.

TSDC together with WP or NIW can be used to analyse the different modes of the DRT on its own. It has been assumed that each mode of the DRT evolves according to its own T_f. This hypothesis allows us to obtain acceptable results. The implications of this hypothesis on the physical mechanism that gives rise to the glass transition are limited due to the phenomenological nature of the approach.

The DSC curves calculated from parameters obtained by the study of the TSDC spectra show a fair agreement with the experimental DSC curves and reproduce the qualitative trends observed when the kinetics of the experiment is changed. Quantitative differences may be due to several reasons that have been discussed in the text.

We have employed two different polarization methods. A comparative analysis between results obtained by the WP and NIW polarization has led us to employ preferentially results obtained from the NIW experiments. There are no major differences between the results obtained by either method but the simpler thermal history of NIW makes its results somewhat more reliable.

TSDC is a method that should be taken into account to study the glass transition. Its main advantage is its capability to study elementary modes of the relaxation. The high resolution of the TSDC spectra is another reason to consider this technique. To sum up, TSDC is a technique worth considering to study the glass transition in polar polymers.

References

[1] McKenna G B 1990 *Comprehensive Polymer Science* vol 2 (*Polymer Properties*) (Oxford: Pergamon) chapter 10, pp 311–58

[2] Ediger M D, Angell C A and Nagel S R 1996 Supercooled liquids and glasses *J. Phys. Chem.* **100** 13200–212

[3] Bernes A, Teyssèdre G, Mezghani S and Lacabanne C 1997 *Dielectric Spectroscopy of Polymeric Materials* (Washington, DC: American Chemical Society) chapter 8, pp 227–58

[4] Schmidt-Rohr K and Spiess H W 1991 Nature of nonexponential loss of correlation above the glass transition investigated by multidimensional NMR *Phys. Rev. Lett.* **66** 3020–3

[5] Schiener B, Chamberlin R V, Diezemann G and Bohmer R 1997 Nonresonant dielectric hole burning spectroscopy of supercooled liquids *J. Chem. Phys.* **107** 7746–61

[6] Sessler G M 1999 *Electrets* vol 2, 3rd edn (Morgan Hill CA: Laplacian) chapter 10, pp 41–80

[7] Hilczer B and Malecki J 1986 *Electrets* (*Studies in Electrical and Electronical Engineering* vol 14) (Warsaw: Elsevier–PWN) chapter 6, pp 285–313

[8] Chen R and Kirsh Y 1981 *Analysis of Thermally Stimulated Processes* 1st edn (Oxford: Pergamon) chapter 3, pp 60–81

[9] Zielinski M and Kryszewski M 1977 Thermal sampling technique for thermally stimulated discharge in polymers–model calculations *Phys. Status Solidi* A **42** 305–14

[10] Sauer B B and Avakian P 1992 Cooperative relaxations in amorphous polymers studied by thermally stimulated current depolarization *Polymer* **33** 5128–42

[11] Teyssèdre G and Lacabanne C 1995 Some considerations about the analysis of thermostimulated depolarization peaks *J. Phys. D: Appl. Phys.* **28** 1478–87

[12] Belana J, Colomer P, Montserrat S and Pujal M 1984–1985 Glass transition temperature of amorphous poly(ethylene terephthalate) by thermally stimulated currents *Macromol. Sci. Phys.* B **23** 467–81

[13] Johari G P and Goldstein M 1970 Viscous liquids and the glass transition. ii. secondary relaxations in glasses of rigid molecules. *J. Chem. Phys.* **53** 2372–88

[14] Johari G P 1973 Intrinsic mobility of molecular glasses *J. Chem. Phys.* **58** 1766–70

[15] Mudarra M and Belana J 1997 Study of poly(methyl methacrylate) space charge relaxation by TSDC *Polymer* **38** 5815–21

[16] Vidal Russell E and Israeloff N E 2000 Direct observation of molecular cooperativity near the glass transition *Nature* **408** 695–8

[17] Moynihan C T, Easteal A J, Wilder J and Tucker J 1974 Dependence of the glass transition temperature on heating and cooling rate *J. Phys. Chem.* **78** 2673–7

[18] Williams G and Watts D C 1970 Non-symmetrical dielectric relaxation behaviour arising from a simple empirical decay function *Trans. Faraday Soc.* **66** 80–5

[19] Cañadas J C, Diego J A, Sellarès J, Mudarra M and Belana J 2000 Cold crystallization effects in free charge relaxation in PET and PEN *Polymer* **41** 8393–400

[20] Bucci C, Fieschi R and Guidi G 1966 Ionic thermocurrents in dielectrics *Phys. Rev.* **148** 816–23

[21] Dargent E, Cabot C, Saiter J M, Bayard J and Grenet J 1996 The glass transition: correlation of TSDC and DSC investigations *J. Therm. Anal. Cal.* **47** 887–96

[22] Press W H, Flannery B P, Teukolsky S A and Vetterling W T 1992 *Numerical Recipes* 2nd edn (Cambridge: Cambridge University Press) chapter 10, pp 387–448

[23] Hodge I M and Berens A R 1981 Calculation of the effects of annealing on sub–T_g endotherms *Macromolecules* **14** 1598–9

[24] Cañadas J C, Diego J A, Mudarra M and Belana J 1998 Comparative TSPC, TSDC and DSC physical ageing studies on PET-a *Polymer* **39** 2795–801